Alanen et al. BMC Musculoskeletal Disorders (2025) 26:423
https://doi.org/10.1186/s12891-025-08652-6

BMC Musculoskeletal Disorders

RESEARCH Open Access

Computer-aided three-dimensional analysis of carpal alignment in scaphoid nonunion advanced collapse wrists: A comparative study with scapholunate advanced collapse and healthy wrists

Mikko Alanen[1*], Samuli Aspinen[1], Theresa Höglund[1], Robert Sippo[1] and Eero Waris[2]

Abstract

Objective To analyze three-dimensional carpal malalignment and height in scaphoid non-union advanced collapse (SNAC) wrists.

Materials and methods Twelve cone-beam CT scans of SNAC wrists were analyzed using computer-aided software to define 3D carpal axes and measure intercarpal angles and carpal height ratio. Comparative data included 121 healthy wrists and 18 wrists with scapholunate advanced collapse (SLAC).

Results SNAC wrists showed dorsal angulation of the lunate and even greater dorsal angulation of the triquetrum, resulting in an increased sagittal scapholunate angle and a decreased sagittal lunotriquetral angle compared to healthy wrists. Compared to SLAC wrists, SNAC wrists had similar sagittal radiolunate and scapholunate angles but a significantly lower lunotriquetral angle. Nonunions in the middle and distal third were associated with greater dorsal angulation of the lunate than proximal third nonunions. In the coronal plane, SNAC wrists showed ulnar tilting of the capitate and hamate compared to healthy wrists. Carpal height ratio was significantly decreased compared with healthy wrists but comparable to SLAC wrists.

Conclusion Scaphoid nonunion location influenced alignment, with proximal nonunions associated with reduced dorsal angulation of the lunate. SNAC wrists differ from SLAC wrists in exhibiting a decreased sagittal lunotriquetral angle, indicating a distinct pathomechanism of carpal instability.

Keywords Angles, Carpal alignment, Computer-aided, Scaphoid fracture, Scaphoid non-union, Scaphoid non-union advanced collapse

*Correspondence:
Mikko Alanen
alanen.mikko.a@gmail.com
[1]Department of Hand Surgery, University of Helsinki and Helsinki University Hospital, Helsinki, Finland
[2]Mehiläinen Helsinki Hospital, Helsinki, Finland

Introduction

Scaphoid fractures carry the risk of nonunion, initiating a progressive sequence of carpal malalignment and degeneration. This malalignment, termed dorsal intercalated segment instability (DISI) [1], is characterized by dorsal angulation of the lunate and proximal scaphoid, while the distal scaphoid angulates palmarly [2]. These changes disrupt carpal kinematics and force distribution, often leading to carpal collapse [3, 4] and osteoarthritis (OA) known as scaphoid non-union advanced collapse (SNAC) [5, 6]. The influence of scaphoid non-union location on the severity of DISI remains inconclusive [2, 7–10]. The SNAC wrists demonstrate a progressive OA pattern, similar to that seen in scapholunate advanced collapse (SLAC) wrists, with a difference that the proximal scaphoid fragment typically remain unaffected by OA changes. In SNAC wrists, degeneration begins at the distal radioscaphoid joint and progresses to the midcarpal joint [5, 6]. Recent studies, however, have questioned the consistency of this OA progression pattern [10, 11].

Current understanding of the carpal pathological deformities relies on visual assessment and manual measurement of carpal angles and distances among the scaphoid, lunate and capitate on lateral radiographs [12, 13]. The advent of cone-beam CT technology and computer-aided analysis, involving segmentation and mathematical modelling, have enabled three-dimensional assessment of carpal alignment and intercarpal relationships, significantly enhancing accuracy and reliability of these evaluations [14–16]. A comprehensive database of three-dimensional carpal alignment and carpal height ratios in 121 healthy wrists has been established [15, 17], with recent studies extending these parameters to SLAC wrists [17].

This study aimed to analyze the three-dimensional carpal malalignment and height ratio in SNAC wrists using computer-aided cone-beam CT analysis. The association between the location of scaphoid non-union and carpal alignment was examined. These findings were compared with previously reported data on healthy wrists [15] and SLAC wrists [17]. We hypothesized that SNAC wrists exhibit distinct carpal alignment patterns compared to healthy and SLAC wrists.

Materials and methods

Image acquisition

To identify the SNAC group, a retrospective chart review of hospital records was conducted for patients who had undergone or were scheduled for a wrist salvage procedure between October 2018 and December 2021. Cases were identified using the Nordic Medico-Statistical Committee (NOMESCO) procedure classifications of Surgical Procedure (NCSP) codes NDG20, NDG00, NDK10 or NDG39, ensuring preoperative wrist cone-beam CT imaging (NCSP codes ND1AI, ND1BI or ND1CI). Medical and radiological records were reviewed to identify patients with scaphoid non-union and radiologically confirmed carpal OA characterized by joint space narrowing at the radioscaphoid, scaphocapitate, lunocapitate and/or triquetrohamate joints. Patients were excluded if they lacked preoperative cone-beam CT scans, were under 18 years old, had rheumatoid arthritis or other inflammatory joint disease, had Kienböck's disease, had a history of wrist trauma other than scaphoid fracture/nonunion, or had undergone prior wrist surgery. Finally, twelve patients (mean age 41.8 years, SD 8.1 range 26.6–56.1) met the inclusion criteria, comprising 11 men and 1 women, with 12 affected wrists (5 right, 7 left). SNAC severity was classified using Vender's grading system as grade 1 in three cases, grade 2 in five cases, and grade 3 in four cases [5]. Scaphoid nonunion was classified by location as distal third in one case, middle third in five cases, and proximal third in six cases [10].

For comparative analysis, two control groups were identified. The SLAC control group included 15 patients (mean age 55.9 years, SD 10.7, range 26.1–73.3, 12 men, 3 women) with 18 SLAC wrists (10 right and 8 left). The SLAC wrists were retrospectively identified alongside with SNAC wrists using the same criteria, except that the history of wrist trauma other than scapholunate dissociation – rather than scaphoid fracture/nonunion – was an exclusion criterion. The medical records and CT scans were reviewed to confirm a widened scapholunate interval and a radiologically verified carpal OA as detailed in a previous study [17].

The healthy control group consisted of prospectively collected data from 121 asymptomatic wrists (61 right and 60 left) of 121 volunteers (mean age 37.7 years, SD 10.4, range 20–60, 69 men, 52 women) who underwent cone-beam CT imaging (Planmed Verity, Planmed Ltd) as previously described [15, 16]. The pseudonymized cone-beam CT scans were exported in Digital Imaging and Communications in Medicine (DICOM) format.

Computer-aided analysis

The computer-aided image analysis software (Bonelogic Hand & Wrist, Disior Ltd, Helsinki, Finland) used in this study processed cone-beam CT scans to automatically generate a patient-specific 3D wrist model by registering numerical 3D models for each bone. Standardized 3D axes were defined for the carpal bones, with specific geometric axes for the distal radius, proximal third metacarpal bone, non-united scaphoid, and capitate [17]. For non-united scaphoid, the software approximated the scaphoid as a single, unified structure despite its division into two fragments. For the lunate, triquetrum and hamate, the normals of the distal articular surface were used, whereas for the trapezium and trapezoideum, the normals of the proximal articular surface were employed

[15]. The computer calculated 3D axes of carpal bones are visualized on Figs. 1a and 1b (Fig. 1). The alignment of these axes were calculated in the sagittal and coronal planes using the radial coordinate system as described in previous studies [15, 18], with palmar and ulnar directions defined as positive. Intercarpal angles were calculated as the difference between distal and proximal radiocarpal angles (sagittal plane) or the ulnar and radial radiocarpal angles (coronal plane). The carpal height ratio, defined as the distance from distal radius articular surface to the distal articular surface of the capitate divided by the distance from the proximal to distal surface of the capitate along its geometric axis, was also calculated as detailed previously [17].

Statistical analysis

Normal distribution of the carpal angle measurement results was confirmed with the Kolmogorov–Smirnov and Shapiro–Wilk tests. Normally distributed data are presented as mean with standard deviation (SD) and range (minimum–maximum). Pearson chi-square test was used to assess whether there were a statistically significant differences in sex and the analyzed wrist side between groups. Student's t-test was used to determine whether there was a statistically significant difference in age between the groups. Pearson correlation (r) was calculated between carpal height ratio and normally distributed continuous variables. Spearman's correlation coefficient (ρ) was calculated between carpal height ratio and non-normally distributed continuous variables. The

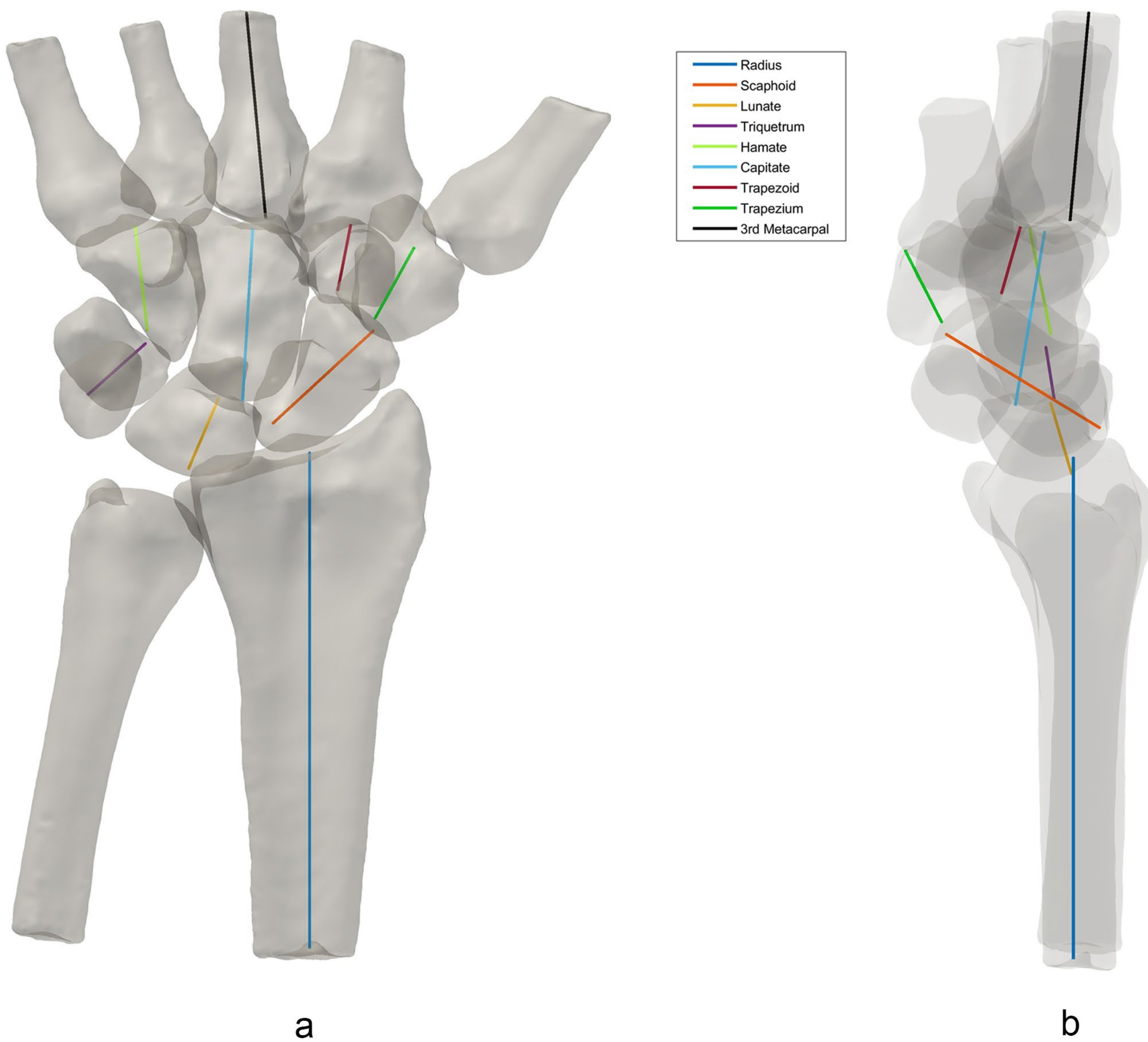

Fig. 1 Presenting the computer calculated 3D axes of carpal bones in posteroanterior (**a**) and lateral (**b**) views

Table 1 Comparison of the sagittal radio- and intercarpal angles among the SNAC, SLAC, and healthy wrist groups

	SNAC	SLAC	Healthy	p1	p2
Radioscaphoid	61 (10; 47 to 79)	68 (11; 42 to 85)	58 (10; 21 to 84)	0.152	0.453
Radiolunate	-28 (9; -43 to -12)	-31 (10; -49 to -14)	0 (11; -27 to 33)	0.634	**< 0.001**
Radiotriquetral	-21 (6; -30 to -8)	-11 (16; -44 to 18)	12 (8; -11 to 27)	0.055	**< 0.001**
Radiotrapezium	6 (10; -13 to 21)	16 (15; -21 to 34)	17 (8; -6 to 32)	0.126	**0.010**
Radiotrapezoid	-19 (12; -42 to -2)	-10 (13; -39 to 9)	-10 (7; -29 to 6)	0.207	0.066
Radiocapitate	-23 (15; -51 to 1)	-24 (14; -50 to -2)	-17 (9; -48 to 2)	0.979	0.496
Radiohamate	3 (14; -16 to 22)	4 (13; -18 to 24)	2 (7; -14 to 22)	0.995	0.993
Radiometacarpal	-7 (11; -25 to 10)	-6 (12; -32 to 9)	-9 (7; -26 to 4)	0.996	0.968
Scapholunate	-89 (16; -118 to -67)	-100 (11; -125 to -76)	-58 (9; -80 to -40)	0.157	**< 0.001**
Lunotriquetral	6 (7; -3 to 19)	20 (11; 1 to 46)	12 (8; -7 to 36)	**< 0.001**	**0.045**
Scaphotrapezium	-55 (9; -66 to -39)	-53 (14; -84 to -28)	-41 (10; -63 to -11)	0.758	**< 0.001**
Scaphotrapezoid	-80 (10; -99 to -69)	-79 (12; -107 to -53)	-67 (9; -89 to -46)	0.915	**< 0.001**
Scaphocapitate	-84 (11; -98 to -62)	-93 (12; -125 to -79)	-74 (11; -99 to -46)	0.074	**0.012**
Lunocapitate	5 (18; -28 to 35)	7 (12; -16 to 32)	-17 (11; -55 to 13)	0.938	**< 0.001**
Lunohamate	31 (18; 7 to 61)	35 (11; 16 to 56)	2 (10; -20 to 27)	0.818	**< 0.001**
Triquetrohamate	24 (16; 4 to 51)	15 (16; -14 to 46)	-10 (7; -23 to 10)	0.339	**< 0.001**
Capitometacarpal	15 (7; 7 to 26)	18 (8; 1 to 34)	8 (6; -4 to 26)	0.435	**< 0.001**
Capitohamate	26 (7; 18 to 41)	29 (7; 13 to 42)	19 (6; 7 to 41)	0.415	**0.001**

Data is presented as the mean (SD; range) in degrees; p1: comparison of results between the SNAC and SLAC groups; p2: comparison of results between groups the SNAC and Healthy wrist goups; Statistically significant p-values are shown in bold

Table 2 Comparison of the coronal radio- and intercarpal angles among the SNAC, SLAC, and the healthy wrist groups

	SNAC	SLAC	Healthy	p1	p2
Radioscaphoid	-40 (9; -57 to -31)	-40 (14; -65 to -17)	-42 (9; -76 to -26)	> 0.90	0.846
Radiolunate	-21 (5; -29 to -13)	-23 (6; -35 to -13)	-20 (4; -32 to -10)	0.549	0.780
Radiotriquetral	-49 (5; -57 to -39)	-52 (6; -35 to -13)	-49 (4; -60 to -39)	0.126	> 0.9
Radiotrapezium	-29 (12; -52 to -14)	-34 (7; -45 to -20)	-32 (6; -43 to -17)	0.582	0.865
Radiotrapezoid	-15 (14; -38 to 7)	-15 (8; -33 to -3)	-16 (5; -28 to -6)	> 0.9	> 0.9
Radiocapitate	11 (11; -11 to 26)	8 (9; -6 to 26)	2 (7; -12 to 23)	0.636	**0.002**
Radiohamate	14 (8; -5 to 24)	8 (5; 1 to 18)	8 (6; -6 to 22)	**0.017**	**0.002**
Radiometacarpal	8 (8; -10 to 19)	2 (6; -7 to 15)	2 (5; -10 to 14)	0.146	0.103
Scapholunate	19 (10; 1 to 37)	18 (14; -2 to 41)	22 (8; 6 to 58)	> 0.9	0.715
Lunotriquetral	-28 (3; -35 to -23)	-30 (6; -38 to -17)	-29 (5, -43 to -18)	0.700	0.422
Scaphotrapezium	11 (13; -20 to 24)	6 (14; -21 to 30)	10 (9; -10 to 43)	0.799	> 0.9
Scaphotrapezoid	25 (14; -3 to 45)	25 (15; -5 to 51)	26 (9; 2 to 60)	> 0.90	> 0.9
Scaphocapitate	51 (13; 25 to 73)	48 (16; 18 to 73)	44 (10; 28 to 90)	> 0.9	0.322
Lunocapitate	32 (9; 17 to 42)	31 (8; 18 to 49)	22 (6; 9 to 40)	> 0.9	**< 0.001**
Lunohamate	35 (8; 18 to 49)	31 (6; 24 to 45)	28 (6; 16 to 42)	0.125	**< 0.001**
Triquetrohamate	63 (7; 47 to 72)	60 (7; 43 to 70)	57 (5; 46 to 71)	0.417	**0.003**
Capitometacarpal	-3 (11; -25 to 14)	-6 (7; -15 to 7)	0 (7; -23 to 12)	0.796	0.819
Capitohamate	4 (12; -21 to 19)	0 (7; -9 to 11)	6 (6; -16 to 19)	0.774	> 0.9

Data is presented as the mean (SD; range) in degrees; p1: comparison of the results between SNAC and SLAC groups; p2: comparison of the results between SNAC and Healthy wrist groups. Statistically significant p-values are shown in bold

correlation coefficients, whether positive or negative, were classified as strong (0.75–1), moderate (0.5–0.75), weak (0.25–0.5), or as no (0–0.25) correlation. A receiver operating characteristics (ROC) curve analysis was plotted for each carpal angle to identify the area under the curve (AUC), and the optimal cut-off value for the prediction SNAC wrist was chosen to be the maximum value of Youden index. A two-tailed p-value < 0.05 was considered statistically significant, 95% confidence intervals were used.

Results

In the SNAC group, there was a significantly higher prevalence of males compared to the healthy wrist group ($p = 0.027$) but there was no difference in gender distribution when compared to the SLAC group ($p = 0.622$). No significant differences were observed in age ($p = 0.117$) or left/right ratio of the imaged wrists ($p = 0.764$) between the SNAC and healthy wrist groups.

Tables 1 and 2 present the sagittal and coronal radio- and intercarpal angles, respectively. No statistically significant differences in sagittal or coronal radiometacarpal angles were observed among the three groups.

Sagittal alignment

In the sagittal plane, the radiocarpal angles of the distal row of carpal bones in the SNAC group did not differ statistically significantly from those of healthy wrists excluding the radiotrapezium angle. No statistically significant difference was found in the radioscaphoid angle between these two groups. In the SNAC group, both the radiolunate and radiotriqueral angles showed more negative values than those observed in the healthy wrist group ($p<0.001$). The scapholunate (SL) angle was more negative in the SNAC group, while the lunotriquetral (LT) angle was decreased compared to the healthy wrist group ($p=0.045$). The lunocapitate, lunohamate and triquetrohamate angles had increased positive values in the SNAC group, while the scaphotrapezial, scaphotrapezoidal and scaphocapitate angles demonstrated increased negative values compared to healthy wrists. The capitometacarpal angle was more positive in the SNAC group than in the healthy wrist group. No statistically significant differences in radio- or intercarpal angles were found between the SNAC and SLAC groups, excluding the LT angle ($p<0.001$). Furthermore, there was a tendency toward a more negative radiotriquetral angle in the SNAC group compared to the SLAC group ($p=0.055$). The AUC and optimal threshold values of sagittal angles indicative for pathologic SNAC process are presented in Table 3.

Coronal alignment

In the coronal plane, no statistically significant differences were observed in radiocarpal angles between the SNAC and healthy wrist groups, excluding the radiocapitate ($p=0.002$) and radiohamate angles ($p=0.002$). Furthermore, there were no significant differences in intercarpal angles within the proximal carpal row, as well as in the capitometacarpal and capitohamate angles between these groups. In the SNAC group, the coronal lunocapitate, triquetrohamate and lunohamate angles were increased in a positive direction compared to the healthy wrist group, but no statistically significant differences were observed in the scaphotrapezial, scaphotrapezoideal and scaphocapitate angles. No statistically significant differences were observed in coronal radio- or intercarpal angles between the SNAC and SLAC groups, excluding the radiohamate angle ($p=0.017$).

Nonunion site

A statistically significant association was observed between the location of the scaphoid nonunion (proximal third vs. distal and middle third) and several sagittal plane angles, including the radiolunate ($p=0.033$), radiotrapezoid ($p=0.034$), SL ($p=0.037$), lunocapitate ($p=0.025$), lunohamate ($p=0.010$), and triquetrohamate ($p=0.027$) angles. In the coronal plane, statistically significant associations were noted between the nonunion location and the radiotrapezoid ($p=0.001$), radiohamate ($p=0.039$), radiometacarpal ($p=0.026$), and scaphotrapezoid ($p=0.022$) angles.

Carpal height ratio

The mean carpal height ratio in the SNAC wrist group was 1.34 (SD 0.11; range 1.13–1.52; CI 95% 1.27–1.40). In SNAC wrists, the carpal height ratio showed a strong correlation with the radiotriquetral angle in the sagittal plane ($r=0.75$, $p=0.005$). It also correlated moderately with several angles in the coronal plane, including the radiocapitate ($r=0.73$, $p=0.008$), lunocapitate (r=-0.71, $p=0.010$), capitometacarpal ($r=0.59$, $p=0.042$), and capitohamate ($r=0.67$, $p=0.017$) angles. (Table 4). The carpal height ratio in the SNAC group was significantly lower

Table 3 The diagnostic value of sagittal radio- and intercarpal angles for SNAC*

Sagittal radio- and intercarpal angles	AUC	95% CI	Optimal Cut-off Value (degrees)*	Sensitivity (%)	Specificity (%)
Radiolunate	0.983	0.961 to 1.000	≤-12	100	89
Radiotriquetral	0.999	0.995 to 1.000	≤ 7	100	98
Radiotrapezium	0.815	0.689 to 0.942	≤ 8	67	90
Scapholunate	0.975	0.944 to 1.000	≤-66	100	85
Lunotriquetral	0.726	0.572 to 0.880	≤ 8	75	72
Scaphotrapezium	0.872	0.769 to 0.975	≤-52	75	90
Scaphotrapezoid	0.826	0.727 to 0,924	≤-71	92	64
Scaphocapitate	0.744	0.599 to 0.890	≤-79	75	70
Lunocapitate	0.862	0.734 to 0.989	≥-8	92	77
Lunohamate	0.940	0.882 to 0.998	≥ 14	92	86
Triquetrohamate	0.997	0.992 to 1.000	≥ 4	100	98
Capitometacarpal	0.806	0.704 to 0.909	≥ 7	100	51
Capitohamate	0.812	0.717 to 0.907	≥ 19	92	65

*) calculated using the Youden index

AUC: area under curve; CI: confidence interval

Table 4 Correlation between carpal height ratio and radiocarpal and intercarpal angles in SNAC wrists

Radio- and intercarpal angle	Sagittal plane	Coronal plane
Radioscaphoid	$r=-0.19$, $p=0.558$	$r=-0.29$, $p=0.370$
Radiolunate	$r=0.44$, $p=0.158$	$r=-0.40$, $p=0.203$
Radiotriquetral	$r=0.75$, $p=0.005$	$r=-0.19$, $p=0.554$
Radiotrapezium	$r=-0.12$, $p=0.708$	$r=-0.27$, $p=0.392$
Radiotrapezoidal	$\rho=-0.273$, $p=0.391$	$r=-0.38$, $p=0.224$
Radiocapitate	$r=-0.10$, $p=0.764$	$r=-0.73$, $p=0.008$
Radiohamate	$r=-0.22$, $p=0.500$	$r=0.00$, $p=0.990$
Radiometacarpal	$r=-0.22$, $p=0.488$	$r=-0.20$, $p=0.531$
Scapholunate	$r=0.39$, $p=0.211$	$r=0.06$, $p=0.851$
Lunotriqueral	$r=0.06$, $p=0.865$	$r=0.35$, $p=0.267$
Scaphotrapezial	$r=0.10$, $p=0.750$	$r=-0.05$, $p=0.876$
Scaphotrapezoideal	$r=-0.09$, $p=0.781$	$r=-0.21$, $p=0.509$
Scaphocapitate	$r=0.07$, $p=0.837$	$r=-0.46$, $p=0.137$
Lunocapitate	$\rho=-0.18$, $p=0.572$	$r=-0.71$, $p=0.010$
Lunohamate	$r=-0.39$, $p=0.207$	$r=0.24$, $p=0.447$
Triquetrohamate	$r=-0.47$, $p=0.125$	$r=0.13$, $p=0.685$
Capitatometacarpal	$r=-0.14$, $p=0.660$	$r=0.59$, $p=0.042$
Capitohamate	$r=-0.22$, $p=0.502$	$r=0.67$, $p=0.017$

Pearson correlation (r) or Spearman's correlation coefficient (ρ) was calculated between carpal height ratio and normally or non-normally distributed continuous variables, respectively. Statistically significant p-values are shown in bold

than that of the healthy wrist group ($p=0.007$) but did not differ significantly from the SLAC group ($p>0.9$).

Discussion

This study demonstrates that in SNAC wrists, the lunate exhibited a dorsal angulation compared to healthy wrists, aligning with previous findings on SL dissociation and SLAC/SNAC pathologies [1, 19]. Notably, the triquetrum showed even greater dorsal angulation than the lunate, resulting in a decreased LT angle in SNAC wrists. In contrast, SLAC wrists showed less triquetral dorsal angulation, leading to an increased sagittal LT angle as previously reported [17]. Thus, in SNAC wrists, the triquetrum appears more prone to dorsal angulation than in SLAC wrists. This difference may be influenced by the dorsal intercarpal ligament (DIC), which attaches to the triquetrum and the distal scaphoid. The intact, palmarly angulated scaphoid in SLAC wrists may restrain triquetral dorsal angulation, while ulnar deviation of the hamate in SNAC wrists may interact with the triquetrum, enhancing dorsal tilt with a corkscrew-like movement.

The geometric axis of the two-part, non-unioned scaphoid showed palmar angulation, consistent with previous findings in DISI deformity and SLAC [17]. However, in this study, the software determined the geometric axis by capturing the two-part scaphoid as a single, unified shape, which can affect the alignment results. Specifically, in SNAC wrists, only the distal scaphoid is palmarly angulated, while the proximal scaphoid tends to angulate dorsally, forming a humback deformity through its connection to the lunate via the SL ligament [7].

The distal carpal row showed a compensatory palmar angulation relative to the lunate and triquetrum, resulting in an increase in the lunocapitate and triquetrohamate angles in the positive direction. These findings are consistent with previously reported data on SLAC pathologies [17]. Additionally, the third metacarpal bone demonstrated a compensatory palmar angulation at the carpometacarpal joint, consistent with recent findings in SLAC wrists [17]. These results indicate that pathologies both in SLAC and SNAC wrists affect not only radio- and midcarpal joints but also secondarily involve the third carpometacarpal joint.

In this study, the sagittal SL, radiolunate and radiotriqueral angles demonstrated the highest AUC values (>0.97) for identifying SNAC wrist malalignment, consistent with previous findings in SL dissociation and SLAC wrists [17, 20, 21]. These results confirm the superior diagnostic utility of these carpal angles in defining both SLAC and SNAC pathologies. Optimal threshold values for SNAC wrist malalignment closely matched those reported for SLAC wrists in recent studies [17, 22]. Specifically, sagittal thresholds were ≤-66° for the SL angle, ≤-12° for the radiolunate angle, and ≥-8° for the lunocapitate angle. To our knowledge, specific threshold values for SNAC malalignment have not been reported in the literature, which typically relies more on the more general DISI pattern as a framework for assessing malalignment. Notably, the LT threshold was ≤8° in SNAC wrists, contrasting with the ≥22° threshold observed in SLAC wrists [17], highlighting distinct triquetral angulation differences between these conditions.

The association between the level of scaphoid nonunions and factors such as displacement, DISI deformity, and degenerative changes has been extensively studied [7–10, 23, 24]. Our study indicates that the proximal scaphoid nonunions are associated with a less pronounced DISI deformity compared to more distal nonunions. These findings are consistent with small case series reported by Morimoto et al. [8] and Oka et al. [7], which suggested a similar trend [7, 8]. Oka et al. (2005) proposed that the development of carpal deformity and subsequent degenerative changes in scaphoid nonunion may depend on whether the fracture line passes distal or proximal to the dorsal apex of the scaphoid ridge, the attachment site of the dorsal scapholunate interosseous ligament. In contrast, studies by Nakamura et al. (1991) and Bulstra et al. (2023) found no association between scaphoid fracture location and DISI deformity or carpal height ratio [23, 24]. Interestingly, some researchers have hypothesized that proximal scaphoid nonunions might lead to more pronounced DISI deformities [2, 9, 10]. Additionally, proximal scaphoid nonunions have also been associated with earlier and more severe OA changes [9, 10]. Notably, a recent study by Bulstra et al. indicated that scaphoid shortening is associated with degree of DISI deformity [24].

In the coronal plane, the axes of proximal carpal row bones in SNAC wrists did not demonstrate statistically significant differences compared to healthy wrists. However, the capitate and hamate showed a significant ulnar tilt in SNAC wrists, consistent with findings from a recent study by Miyamora et al. [11]. Interestingly, this pattern contrasts with SLAC wrists, where only the capitate demonstrated ulnar tilt, while the hamate remained unchanged in the coronal plane [17]. This difference may be attributed to the earlier speculated more tense DIC ligament in SLAC wrists, which could allow greater triquetral angulation in SNAC wrists. Such dorsal angulation of triquetrum might create more space for both the hamate and capitate enabling the ulnar tilt of them. An alternative explanation involves differences in shear forces at the capitohamate joint. In SLAC wrists, the capitate protrudes into the SL gap [25] creating a shearing force between the capitate and hamate that restricts the hamate's ability to tilt ulnarly. In SNAC wrists, the capitate may protrude proximally to lesser extent due to the presence of proximal scaphoid fragment. This reduced protrusion permits greater sliding motion of both the capitate and hamate along the second Gilula's line. This hypothesis is further supported by the tendency for a greater coronal radiocapitate and radiohamate angle observed in SNAC wrists.

The carpal height ratio, a measure of carpal collapse [17, 26] averaged 1.34 in our study of SNAC wrists, compared to a higher mean value of 1.47 in healthy wrists. This ratio was comparable with the previously reported carpal height ratio of 1.33 for SLAC wrists [17], indicating comparable levels of carpal collapse in these two pathologies. The optimal cut-off value for identifying malalignment in SNAC wrists was determined to be 1.37, with a sensitivity of 67% and specificity of 90%. Among all radio- and intercarpal angles, the carpal height ratio showed a strong correlation with triquetrum dorsal angulation and a moderate correlation with capitate ulnar deviation, highlighting these specific carpal bone movements as primary contributors to collapse in SNAC wrists. Interestingly, the carpal height ratio showed no statistically significant correlation with sagittal radiolunate or capitolunate angles.

Standardized measurement techniques and imaging protocols are essential for accurate and reliable assessment of carpal alignment [14, 18]. The computer-aided technique offers an automated, highly accurate and reliable evaluation of 3D carpal alignment from CT and MRI images [14–16]. Cone-beam CT scanning enables neutral wrist positioning, while digital determination of the coronal and sagittal planes minimizes projection variability. Integrating automated carpal alignment analysis into clinical practice could improve diagnostic accuracy by highlighting abnormal values, reducing interpretation time, and minimizing errors. This study enhances understanding of the mechanisms underlying scaphoid nonunion related carpal instability and degeneration. Carpal malalignment in SNAC wrists alters kinematics and load distributions, often leading to pain, decreased motion and osteoarthritic changes. Segmentation and numerical modeling of CT and MRI data allows joint surface distance distribution analysis using distance mapping [27]. Ongoing studies focus on developing software for the automated quantification of wrist osteoarthritis severity and extent.

This study has several limitations. The retrospective design may introduce selection bias, and the sample size was relatively small with only one SNAC wrist featuring a distal third nonunion. Furthermore, only SNAC wrists scheduled for salvage procedures were included, which may have biased the selection toward more advanced SNAC stages; however, the distribution of SNAC stages remained in our study relatively balanced based on Vender's classification. The two-part, non-united scaphoid was analyzed as whole for axis determination. Further studies will aim to separately determine the axes of the proximal and distal fragments, allowing for a more detailed analysis of alignment in scaphoid fractures and non-unions.

In conclusion, SNAC wrists showed dorsal angulation of the lunate and triquetrum, with greater angulation in the triquetrum, leading to a decreased sagittal LT angle. In contrast, SLAC wrists have less triquetrum angulation and increased LT angle. To compensate for the dorsal angulation of the lunate and triquetrum, both the distal carpal row and third metacarpal exhibited palmar angulation. In the coronal plane, ulnar tilting of the capitate and hamate contributed further to malalignment. Collectively, these changes resulted in carpal collapse. The location of the scaphoid nonunion influenced carpal malalignment, with proximal nonunion being associated with reduced dorsal angulation of the lunate. Further studies are needed to elucidate how these alignment changes affect carpal kinematics, load distribution, and degeneration progression.

Acknowledgements

The authors thank Disior Ltd for developing the software, Planmed Ltd for providing facilities for imaging, and Pasi Ohtonen for conducting the statistical analysis.

Author contributions

MA researched the literature, collected and analyzed the data and wrote the manuscript. EW conceived the study, analyzed the data, and wrote the manuscript. SA contributed to study design and methodology. TH and RS were involved in volunteer recruitment. All authors reviewed and edited the manuscript and approved the final version of the manuscript.

Funding
Open Access funding provided by University of Helsinki (including Helsinki University Central Hospital).
The author(s) disclosed receipt of the following financial support for the research, authorship, and/or publication of this article: This work was supported by the University of Helsinki and Helsinki University Hospital, the Finnish Medical Foundation, and Vappu Uuspää foundation.

Data availability
The datasets used and/or analysed during the current study are available from the corresponding author on reasonable request.

Declarations

Ethical approval and consent to participate
The ethics committee of Helsinki University Central Hospital (HUS/147/2019, HUS/1717/2019) and institutional review board reviewed and approved the study in accordance with the Declaration of Helsinki. Written informed consent was obtained from the volunteers to participate to study.

Consent for publication
Written informed consent was obtained from the volunteers for their anonymized information to be published in this article.

Competing interests
The authors declared the following potential conflicts of interest with respect to the research, authorship, and/or publication of this article: E.W. has owned stock in Disior Ltd, Helsinki, Finland and sold them in January 2022. The other authors have no conflicts of interest to declare.

Received: 15 February 2025 / Accepted: 14 April 2025
Published online: 29 April 2025

References
1. Braun S, Berger N, Wolfe RA. Defining DISI and VISI. J Hand Surg Eur Vol. 2021;46(5):566–8. https://doi.org/10.1177/1753193421989933.
2. Kompoliti E, Prodromou M, Karantanas AH, SLAC, Wrist SNAC. The top five things that general radiologists need to know. Tomography. 2021;7(4):488–503. https://doi.org/10.3390/tomography7040042.
3. Mack GR, Bosse MJ, Gelberman RH, Yu E. The natural history of scaphoid non-union. J Bone Joint Surg Am. 1984;66(4):504–9. PMID: 6707028.
4. Allende BT. Osteoarthritis of the wrist secondary to non-union of the scaphoid. Int Orthop. 1988;12(3):201–11. https://doi.org/10.1007/BF00547164.
5. Vender MI, Watson HK, Wiener BD, Black DM. Degenerative change in symptomatic scaphoid nonunion. J Hand Surg Am. 1987;12(4):514–9. https://doi.org/10.1016/s0363-5023(87)80198-3.
6. Watson HK, Brenner LH. Degenerative disorders of the wrist. J Hand Surg Am. 1985;10(6 Pt 2):1002–6. https://doi.org/10.1016/s0363-5023(85)80025-3.
7. Oka K, Moritomo H, Murase T, Goto A, Sugamoto K, Yoshikawa H. Patterns of carpal deformity in scaphoid nonunion: a 3-dimensional and quantitative analysis. J Hand Surg Am. 2005;30(6):1136–44. https://doi.org/10.1016/j.jhsa.2005.08.004.
8. Moritomo H, Viegas SF, Elder KW, Nakamura K, Dasilva MF, Boyd NL, Patterson RM. Scaphoid nonunions: a 3-dimensional analysis of patterns of deformity. J Hand Surg Am. 2000;25(3):520–8. https://doi.org/10.1053/jhsu.2000.7381.
9. Dias JJ, Kheiran A, Ngo DN, Adeleye E, Wildin CJ, Ullah A, Bhowal B, Bindra R. The onset, progress and factors influencing degenerative arthritis of the wrist following scaphoid fracture non-union. Injury. 2023;54(3):930–9. https://doi.org/10.1016/j.injury.2022.12.025.
10. Crema MD, Phan C, Miquel A, Quach C, Arrivé L, Menu Y. MDCT arthrography assessment of scaphoid nonunion advanced collapse: distribution of cartilage damage and relationship with scaphoid nonunion features. Skeletal Radiol. 2018;47(8):1157–65. https://doi.org/10.1007/s00256-018-2907-7.
11. Miyamura S, Shiode R, Lans J, Oka K, Tanaka H, Okada S, Murase T, Chen NC. Quantitative 3-D CT demonstrates distal row pronation and translation and radiolunate arthritis in the SNAC wrist. J Bone Joint Surg Am. 2023;105(17):1329–37. https://doi.org/10.2106/JBJS.22.01350.
12. Selles CA, Ras L, Walenkamp MMJ, Maas M, Goslings JC, Schep NWL. Carpal alignment: A new method for assessment. J Wrist Surg. 2019;8(2):112–7. https://doi.org/10.1055/s-0038-1673406.
13. Larsen CF, Stigsby B, Lindequist S, Bellstrøm T, Mathiesen FK, Ipsen T. Observer variability in measurements of carpal bone angles on lateral wrist radiographs. J Hand Surg Am. 1991;16(5):893–8. https://doi.org/10.1016/s0363-5023(10)80157-1.
14. Sippo R, Huuska K, Höglund T, Waris E. Comparison of computer-aided and manual measurements in the evaluation of carpal alignment. J Hand Surg Eur Vol. 2024;49(8):987–94. https://doi.org/10.1177/17531934231220637.
15. Höglund TEK, Sippo RMJ, Waris E. Three-dimensional carpal alignment: computer-aided CT analysis of carpal axes and normal ranges. J Hand Surg Eur Vol. 2023;48(8):792–7. https://doi.org/10.1177/17531934231160100.
16. Sippo RMJ, Höglund TEK, Waris E. Computer-based three-dimensional measurement of carpal alignment: measurement techniques and normal ranges. J Hand Surg Eur Vol. 2021;46(10):1064–71. https://doi.org/10.1177/17531934211039661.
17. Alanen M, Aspinen S, Höglund T, Sippo R, Waris E. Comparative Computer-Aided analysis of Three-Dimensional carpal alignment in scapholunate advanced collapse and healthy wrists. J Hand Surg Am. 2024 Nov;14(24):S0363–5023. https://doi.org/10.1016/j.jhsa.2024.09.021.
18. Suojärvi N, Tampio J, Lindfors N, Waris E. Computer-aided 3D analysis of anatomy and radiographic parameters of the distal radius. Clin Anat. 2021;34(4):574–80. https://doi.org/10.1002/ca.23615.
19. Omori S, Moritomo H, Omokawa S, Murase T, Sugamoto K, Yoshikawa H. In vivo 3-dimensional analysis of dorsal intercalated segment instability deformity secondary to scapholunate dissociation: a preliminary report. J Hand Surg Am. 2013;38(7):1346–55. https://doi.org/10.1016/j.jhsa.2013.04.004.
20. Pliefke J, Stengel D, Rademacher G, Mutze S, Ekkernkamp A, Eisenschenk A. Diagnostic accuracy of plain radiographs and cineradiography in diagnosing traumatic scapholunate dissociation. Skeletal Radiol. 2008;37(2):139–45. https://doi.org/10.1007/s00256-007-0410-7.
21. Dornberger JE, Rademacher G, Mutze S, Eisenschenk A, Stengel D. Accuracy of simple plain radiographic signs and measures to diagnose acute scapholunate ligament injuries of the wrist. Eur Radiol. 2015;25(12):3488–98. https://doi.org/10.1007/s00330-015-3776-2.
22. Megerle K, Pöhlmann S, Kloeters O, Germann G, Sauerbier M. The significance of conventional radiographic parameters in the diagnosis of scapholunate ligament lesions. Eur Radiol. 2011;21(1):176–81. https://doi.org/10.1007/s00330-010-1910-8.
23. Nakamura R, Imaeda T, Horii E, Miura T, Hayakawa N. Analysis of scaphoid fracture displacement by three-dimensional computed tomography. J Hand Surg Am. 1991;16(3):485–92. https://doi.org/10.1016/0363-5023(91)90019-8.
24. Bulstra AEJ, Vidovic AJ, Doornberg JN, Jaarsma RL, Buijze GA. Scaphoid length loss following nonunion is associated with dorsal intercalated segment instability. J Wrist Surg. 2023;12(5):407–12. https://doi.org/10.1055/s-0043-1760753.
25. Bathala EA, Bancroft LW. The case: scapholunate advanced collapse (SLAC wrist). Orthopedics. 2007;30(6):418. https://doi.org/10.3928/01477447-20070601-14.
26. Nattrass GR, King GJ, McMurtry RY, Brant RF. An alternative method for determination of the carpal height ratio. J Bone Joint Surg Am. 1994;76(1):88–94. https://doi.org/10.2106/00004623-199401000-00011.
27. Siegler S, Konow T, Belvedere C, Ensini A, Kulkarni R, Leardini A. Analysis of surface-to-surface distance mapping during three-dimensional motion at the ankle and subtalar joints. J Biomech. 2018;76:204–11. https://doi.org/10.1016/J.JBIOMECH.2018.05.026.

Publisher's note